THE EVOLVING OBSCURED AGN POPULATION AND THE COSMIC X-RAY BACKGROUND

R. Gilli[1], A. Comastri[1], and G. Hasinger[2]

[1]INAF - Osservatorio Astronomico di Bologna, via Ranzani 1, 40127, Bologna, Italy
[2]Max-Planck-Institut für extraterrestrische Physik, Postf. 1312, 85741 Garching, Germany

ABSTRACT

We present a new modeling of the cosmic X-ray background (XRB) based on the most up-to-date AGN X-ray luminosity functions (XLF) and evolution. The most recent results from the soft (0.5-2 keV) and hard (2-10 keV) X-ray surveys are used to constrain at best the contribution of Compton-thin AGN to the XRB. In particular, the ratio between moderately obscured AGN (Compton-thin) and unobscured AGN is estimated directly by comparing the soft and hard XLF. This comparison suggests that the fraction of obscured AGN decreases with intrinsic luminosity. The model is in agreement with the soft and hard AGN counts over about 6 dex in flux. A large population of heavily obscured -Compton thick- AGN is added to fit the XRB spectrum above 10 keV. Remarkably, the fraction of Compton thick AGN observed in the Chandra Deep Field South is in excellent agreement with that predicted by the model.

Key words: galaxies:active - X-rays:general.

1. INTRODUCTION

The deepest X-ray surveys in the Lockman Hole (Hasinger 2004), Chandra Deep Field South (Giacconi et al. 2002) and Chandra Deep Field North (Alexander et al. 2003) have shown that most of the cosmic X-ray background below 10 keV is resolved into discrete sources (e.g. Worsley et al. 2005), the vast majority of which have been identified as active galactic nuclei (e.g. Szokoly et al. 2003, Barger et al. 2003). The combination of deep with shallower surveys has allowed to construct the AGN X-ray luminosity function both in the soft 0.5-2 keV band (Hasinger et al. 2005) and in the hard 2-10 keV band (Ueda et al. 2003, La Franca et al. 2005) and map the evolution of X-ray selected AGN up to redshifts of $z \sim 5$. Although X-ray observations are less biased towards obscured AGN, sensitive imaging survey can be performed at present only at energies below 10 keV. Therefore, they are expected to severely undersample the population of extremely obscured AGN with column densities above $logN_H = 24$ (i.e. Compton-thick sources) which, at least in the local Universe, are found to be as numerous as moderately obscured AGN (Risaliti et al. 1999; Guainazzi et al. 2005), and are expected to provide a significant contribution to the 30 keV peak in the XRB spectrum (Comastri et al. 1995; Gilli et al. 2001).

2. THE MODEL

In our modeling we tightly constrain the properties of Compton-thin AGN, for which a large body of observational data (e.g. source counts, luminosity functions and redshift distributions) are available. Once the population of Compton-thin AGN is fully characterized, we compute their contribution to the XRB spectrum and add as many Compton thick AGN as needed to fit the XRB spectrum above 10 keV, in particular the XRB bump at 30 keV. We remark that at $E < 10$ keV different instruments have measured different XRB intensities, with variations as large as 40% (the lower and higher value being measured by HEAO-1 and BeppoSAX, respectively), while in the energy range 10-300 keV the HEAO-1 measurement is still the only available one (see Gilli 2004 and Revnivtsev et al. 2005 for recent discussions). Since the discrepancies in the XRB measurements are not fully understood, we will not adopt the XRB below 10 keV as a primary constraint. Rather we rely on what we believe to be more robust observational data such as the 0.5-2 keV and 2-10 keV logN-logS and luminosity functions and verify *a posteriori* the resulting XRB spectrum.

More specifically the adopted strategy is as follows:

we assume that surveys in the 0.5-2 keV band are essentially tracing the population of unobscured ($\log N_H < 21$) AGN, while surveys in the 2-10 keV band are tracing the population of unobscured plus Compton thin ($\log N_H < 24$) AGN. Therefore the moderately obscured AGN population can be reasonably well estimated as the difference between the hard (total) and soft (unobscured) XLF.

It is well known (e.g. Comastri et al. 1995) that the

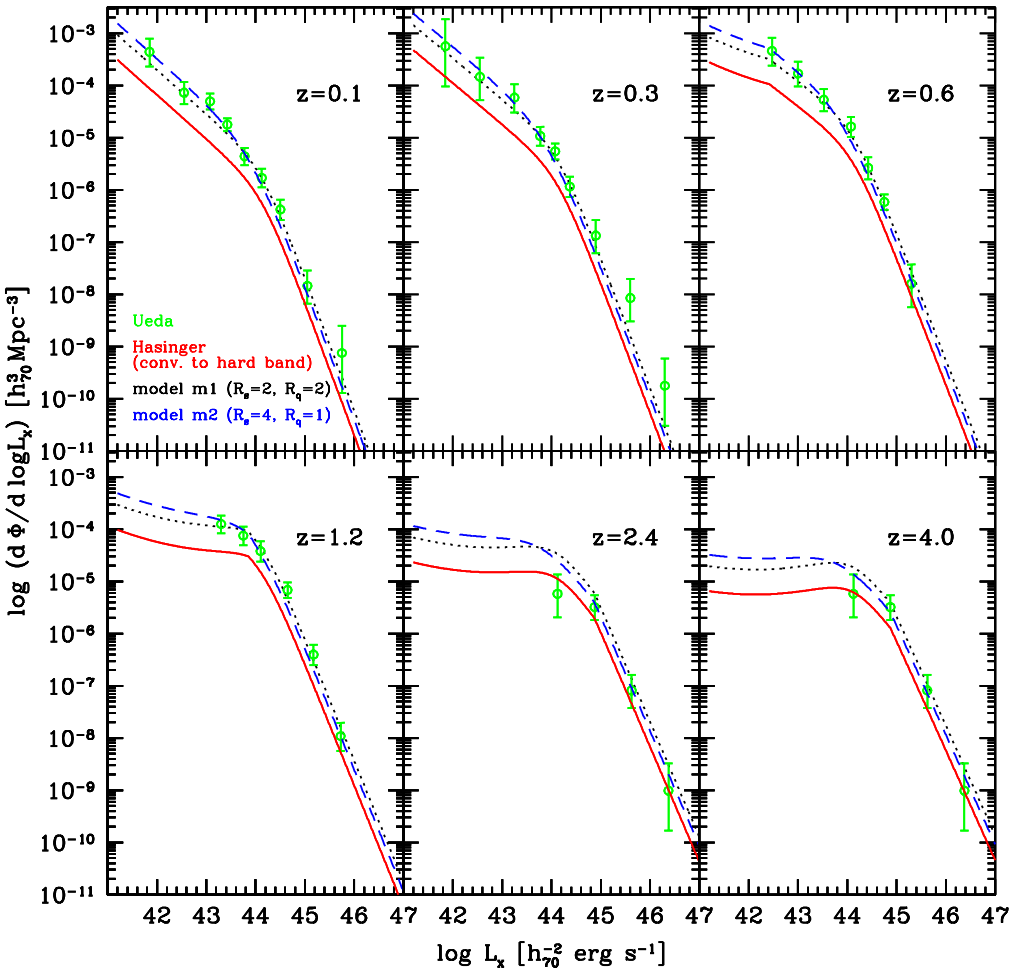

Figure 1. The Ueda et al. (2003) intrinsic hard XLF for the total Compton-thin AGN population (datapoints) compared with models m1 (dotted line) and m2 (dashed line). The soft XLF by Hasinger et al. (2005) converted to the hard band is also shown (solid line).

source counts in the hard X-ray band cannot be matched by simply converting the soft counts to the hard band assuming a standard unabsorbed AGN spectrum (e.g. a powerlaw with photon index $\Gamma = 1.9$). Similarly (Fig. 1), converting the soft XLF by Hasinger et al. (2005) to the hard band (assuming $\Gamma = 1.9$) is not sufficient to reproduce the total hard XLF, so obscured AGN have to be added.

We introduce the ratio R between obscured Compton-thin AGN and unobscured AGN (i.e. the number ratio between sources with $21 < logN_H < 24$ and with $logN_H < 21$) defined as follows:

$$R = R_S\, e^{-L/L_s} + R_Q\, (1 - e^{-L/L_s}), \qquad (1)$$

where R_S is the ratio in the Seyfert (low-) luminosity regime and R_Q is the ratio in the QSO (high-) luminosity regime, and L_s is the 0.5-2 keV characteristic luminosity dividing the two regimes (we fixed $logL_s = 43.5$). The total AGN hard XLF is simply obtained by converting the soft (unobscured) XLF to the hard band and then multiplying it by (1+R).

We considered two hypotheses: first (model m1) we assumed a ratio independent of luminosity where $R = R_Q = R_S = 2$; second (model m2), we assumed $R_S = 4$ and $R_Q = 1$ to account for a decline in the obscured AGN fraction with luminosity as suggested by several observational results (e.g. Ueda et al. 2003, La Franca et al. 2005).

As shown in Fig. 1, both models match the hard XLF by Ueda et al. (2003), however model m2 seems to provide a better description of the data than model m1. The recent hard XLF estimated by La Franca et al. (2005) lends further support to such a possibility (see Fig. 2). Therefore

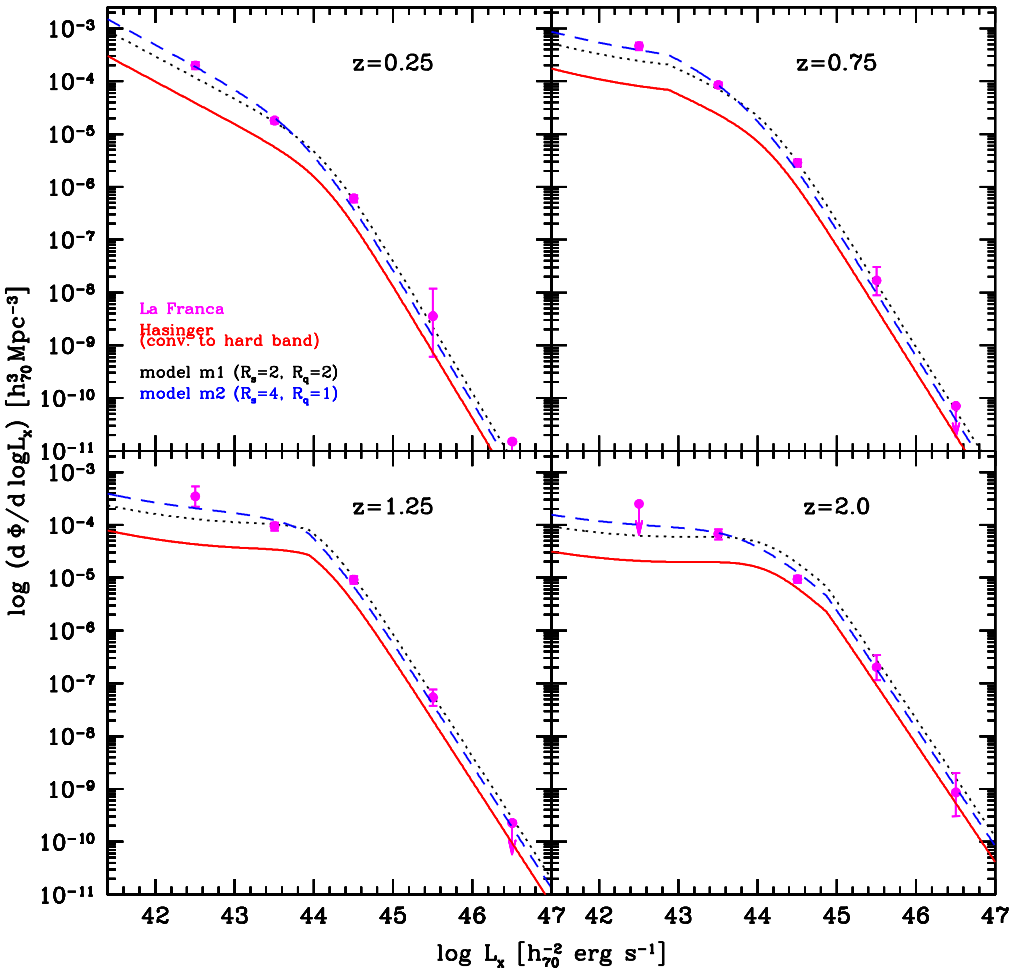

Figure 2. Same as the previous Figure but considering the hard XLF data of La Franca et al. (2005).

model m2 will be considered as our baseline model in the following.

It is worth noting that the comparison between the soft and hard XLF allows to constrain the total number of obscured Compton-thin AGN with no assumptions on their column density distribution. The latter is estimated by considering the soft and hard cumulative number counts as explained below. We divided Compton-thin sources into three absorption bins centered at $logN_H = 21.5, 22.5, 23.5$. Following previous studies (Comastri et al. 1995, Risaliti et al. 1999, Gilli et al. 2001), the number of sources in each bin is chosen to increase with obscuration from $logN_H = 21.5$ to $logN_H = 23.5$ in order to reproduce the AGN counts in the soft and hard band over about 6 orders of magnitude in flux (Fig.3 and 4, respectively). A flat N_H distribution overpredicts the soft X-ray counts at faint fluxes and appears to be disfavored.

At this stage we believe that the population of moderately obscured sources is well constrained and their contribution to the XRB spectrum is computed (Fig. 5). A cut off powerlaw with photon index $\Gamma = 1.9$ and e-folding energy $E_c = 320$ keV is assumed as an input template for unabsorbed AGN. Absorption by different column densities is then introduced to model the spectra of obscured sources. A Compton reflection component is also added to the spectrum of AGN in the Seyfert luminosity regime, with a different normalization for obscured and unobscured sources (see Comastri et al. 1995).

The integrated emission of this population is found to explain most of the XRB below 10 keV as measured by HEAO-1 (see Fig. 5), but, as expected, fails to reproduce the 30 keV bump, calling for an additional population of Compton-thick sources. In our modeling these were divided into two, equally populated, absorption bins with $logN_H = 24.5$ and $logN_H > 25$, where distinct spectral templates have been considered according to the different physical scenarios: in the first case the direct, transmitted emission is still the main component above $\sim$ 10 keV, while at lower energies, where this is heavily absorbed,

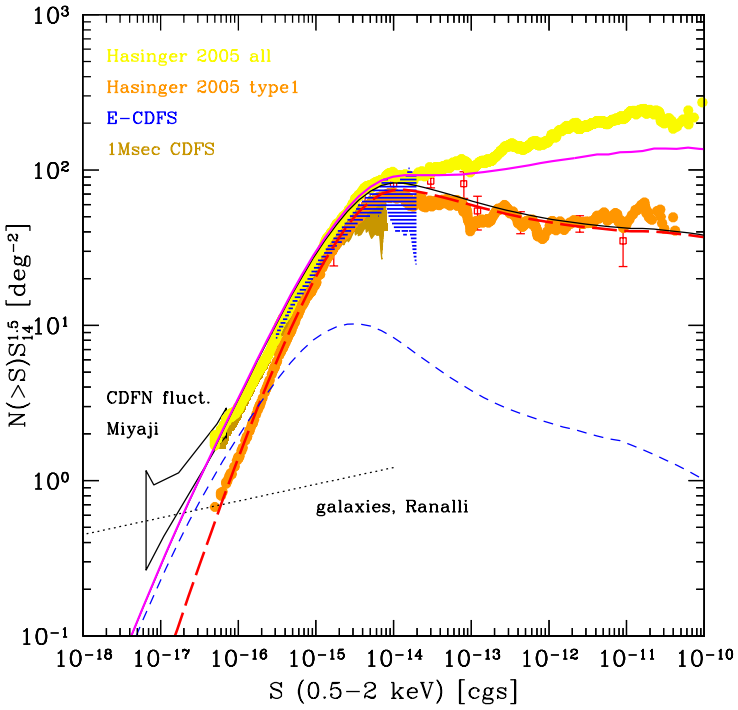

Figure 3. Cumulative soft AGN counts normalized to an Euclidean Universe. Datapoints are explained on the top left. The model curves for unabsorbed AGN, absorbed AGN, total AGN, and total AGN + clusters are shown respectively with the following line styles: red long-dashed, blue short-dashed, solid black, solid magenta. At bright fluxes the data are not cleaned by Galactic sources, thus producing an apparent discrepancy wrt the total model prediction.

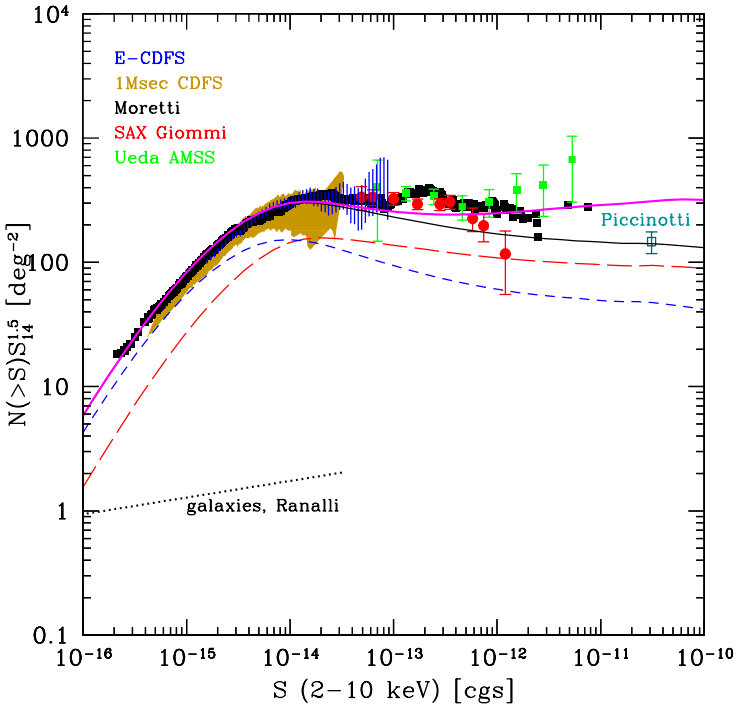

Figure 4. Cumulative hard AGN counts normalized to an Euclidean Universe. Datapoints are explained on the top left. The model curves and corresponding line styles are as in the previous Figure.

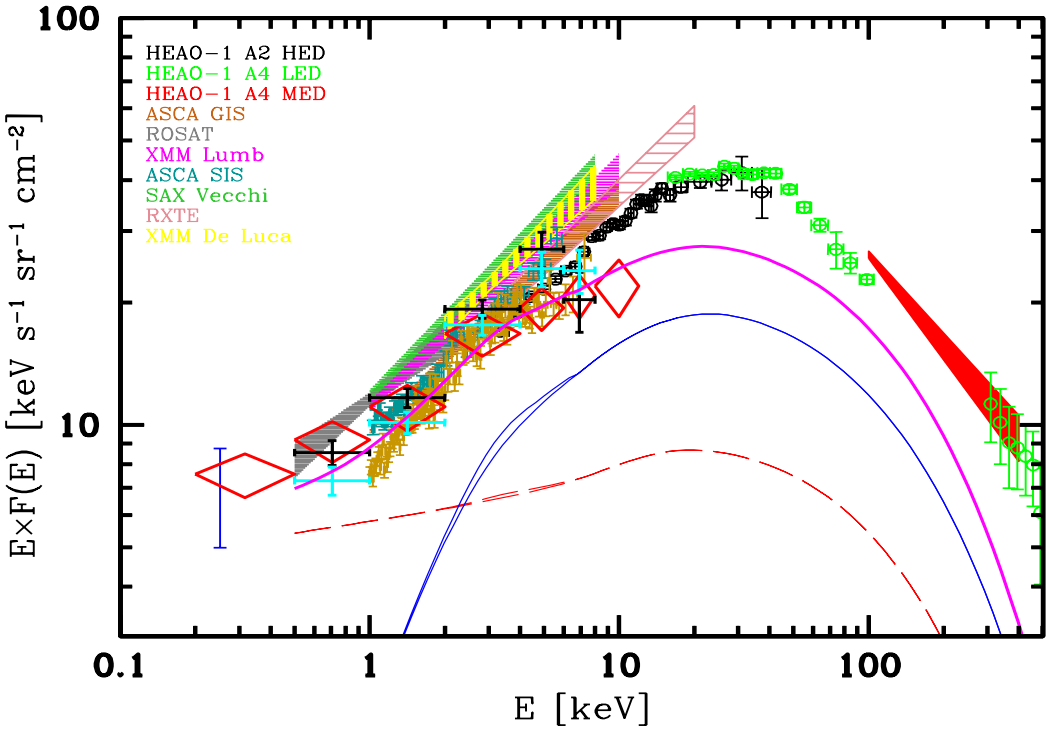

Figure 5. The cosmic XRB spectrum and predicted contribution from the population of Compton-thin AGN. The different XRB measurements are explained on the top left. Also shown are the resolved XRB fractions in different surveys by Worsley et al. (2005): Lockman Hole = red diamonds; CDFS = cyan crosses; CDFN = black crosses. Curves refer to model m2: unobscured AGN = red long-dashed line; obscured Compton thin AGN = blue short-dashed line; total (also including galaxy clusters) = magenta solid line.

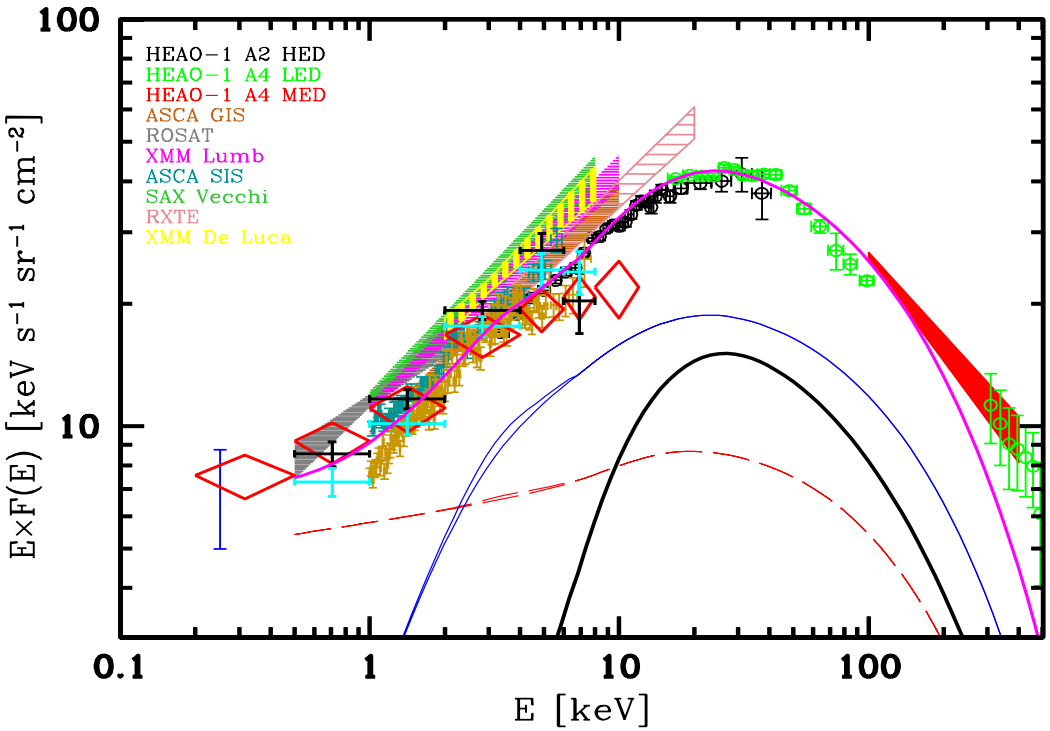

Figure 6. Same as in the previous Figure but with the additional contribution of Compton-thick sources (thick black line).

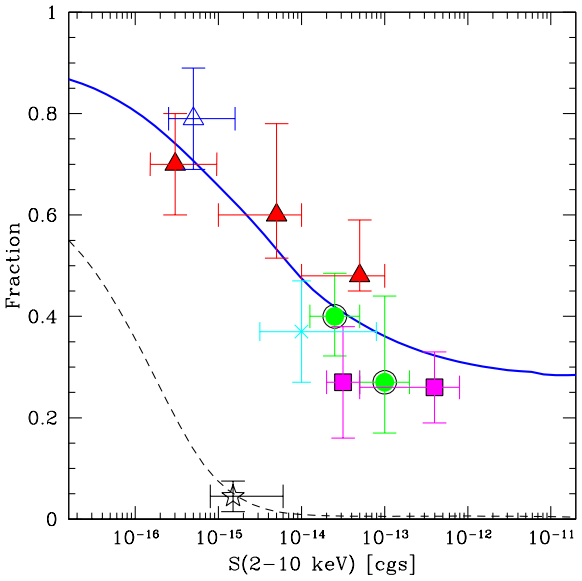

Figure 7. The fraction of obscured AGN as a function of the 2-10 keV limiting flux. Solid blue line: fraction of AGN with $logN_H > 22$ expected by model m2. Colored points: fraction of AGN with $logN_H > 22$ measured in different surveys (datapoints are described in Gilli et al. 2006 in prep). Black dashed line: fraction of AGN with $logN_H > 24$ (i.e. Compton-thick) expected by model m2. Black star: fraction of Compton-thick AGN measured in the CDFS by Tozzi et al. (2005).

the reflected continuum (e.g. by the far inner side of the putative obscuring torus) provides a major contribution; in the second case absorption is extreme and no radiation is transmitted through the absorber, leaving a bare reflection continuum as the only visible component.

As shown in Fig. 6, the fit to the XRB spectrum measured by HEAO-1 in the range 10-300 keV requires a large number of Compton thick AGN (about twice as large as that of Compton-thin one). An even larger Compton-thick population would be required if the XRB flux were underestimated by HEAO-1.

The baseline model nicely reproduces the steep rising of the obscured AGN fraction as a function of hard limiting flux as estimated by several surveys (Fig. 7). Remarkably, the model predicted fraction of Compton-thick AGN closely matches the small ($\sim 5\%$) observed fraction of heavily obscured sources measured by Tozzi et al. (2005) in the Chandra Deep Field South (see again Fig. 7). Our results confirm that below 10 keV the large population of Compton thick sources is poorly sampled even by the deepest surveys.

ACKNOWLEDGMENTS

REFERENCES

Alexander, D.M., Bauer, F.E., Brandt, W.N., et al. 2003, AJ, 126, 539

Barger, A.J., Cowie, L.L., Capak, P., et al. 2003, AJ, 126, 632

Comastri, A., Setti, G., Zamorani, G., & Hasinger, G. 1995, A&A, 296, 1

Giacconi, R., Zirm, A., Wang, J., et al. 2002, ApJS, 139, 369

Gilli, R., Salvati, M., & Hasinger, G. 2000, A&A, 366, 407

Gilli, R. 2004, Ad. Sp. Res., 34, 2470

Guainazzi, M., Matt, G., Perola, G.C. 2005, A&A, in press (astro-ph/0508265)

Hasinger, G. 2004, Nuc. Phys. B Proc. Supp., 132, 86

Hasinger, G., Miyaji, T., Schmidt, M. 2005, A&A, 441, 417

La Franca, F., Fiore, F., Comastri, A., et al. 2005, ApJ, in press (astro-ph/0509081)

Revnivtsev, M., et al. 2005, A&A, in press (astro-ph/0412304)

Tozzi, P., Gilli, R., Mainieri, V., et al. 2005, A&A, in press

Ueda, Y., Akiyama, M., Ohta, K., Miyaji, T. 2003, ApJ, 598, 886

Worsley, M.A., Fabian, A.C., Bauer, F.E., et al. MNRAS, 2005, 357, 1281